

Dynamic Characteristics of a 30-cm Mercury Ion Thruster

J. S. Serafini,* M. A. Mantenicks,† and V. K. Rawlin†
NASA Lewis Research Center, Cleveland, Ohio

Fluctuations of the discharge and beam plasmas of a 30-cm ion thruster have been measured using 60-Hz laboratory-type power supplies. The thruster was operated at beam currents of 2.0, 1.5, and 1.0 A over a range of magnetic baffle currents, at constant discharge power and voltage. The time-varying properties of the discharge voltage and current, the ion beam current, and the neutralizer keeper current were measured. The intensities of the fluctuations (ratio of the rms magnitude to time-average quantity) were found to depend significantly on the beam and magnetic baffle currents. The predominant peaks of the beam and discharge current spectra occurred at frequencies less than 30 kHz. Cross-correlations of the discharge and beam currents indicated that the dependence on the magnetic baffle current was strong.

Nomenclature

A_0	= relative amplitude of peak occurring at fundamental frequency, dimensionless
A_1, A_2, \dots	= relative amplitude of peaks at first, second, ... harmonic frequencies, dimensionless
F_0	= fundamental frequency, kHz
F_1, F_2, \dots	= first, second, ... harmonic frequencies, kHz
f	= frequency, Hz
$J(t)$	= $\bar{J}(t) + j(t)$; sum of time-average and time-varying currents, A
$J_B(t)$	= beam current, A
$J_I(t)$	= discharge current, A
J_{MB}	= magnetic baffle current, A
$J_{NK}(t)$	= neutralizer keeper current, A
$j(t)$	= time-varying current, A
R	= correlation coefficient as a function of τ , the time-delay
R_{\max}	= maximum correlation coefficient
$\Delta V_I(t)$	= $\Delta V_I(t) + \Delta V_I(t)$; sum of time-mean and time-varying discharge voltages, V
$\Delta v_I(t)$	= time-varying discharge voltage, V
τ	= time-delay between two fluctuations
$'$	= fluctuation intensity defined as ratio of rms magnitude to time-average i.e., $j'_B = (\bar{j}_B^2 / \bar{J}_B)^{1/2}$
—	= overbar denotes time average of a physical quantity

Introduction

THE 30-cm-diam ion thruster is being considered for primary propulsion applications for Earth orbital and interplanetary missions.¹⁻³ In these applications, electrical noise or fluctuations are of concern.^{4,5} The operation of a mercury electron bombardment thruster can yield fluctuations about the mean current and potential of the ion beam, fluctuations of the discharge plasma, and fluctuations within the power conditioner itself. In addition, information on these fluctuations could aid in optimizing performance and life of the thruster and power supplies. The present paper is a continuation of the work presented in Ref. 6. The present work reports on measurements of the fluctuations in the beam current, neutralizer keeper current, discharge current, and

discharge voltage. A range of beam current and magnetic baffle current values and discharge chamber conditions was covered in the investigation. Several properties of the fluctuations were recorded using the techniques of Refs. 7-9.

Apparatus and Experimental Technique

A 30-cm-diam mercury bombardment ion thruster built by Hughes Research Laboratories was used for the tests described herein. It was a "400 series" thruster modified to be nominally equivalent to the Engineering Model Thruster described in Ref. 10 and the same thruster used in Ref. 11. The magnetic baffle control coil had 3.5 turns. The baffle diameter used was 5.08 cm except when otherwise mentioned. The thruster was operated in the 3.0 m-diam port of the 7.6-m-diam by 21.4 m-long vacuum facility at Lewis Research Center.¹² Laboratory-type power supplies powered from the 60-Hz line were used to operate the thruster. Additional details on the power supplies and the filtering are given in Ref. 13.

The thruster always was operated with net and total accelerating voltages of 1100 and 1600 V, respectively. The discharge losses were fixed at 185 eV per beam ion for all beam currents. The beam current was varied by adjusting the main propellant flow to the thruster, and beam currents of 1.0, 1.5, and 2.0 A were used in the tests. The discharge voltage was maintained constant at 37.0 V by adjusting the mercury flow through the cathode. For any given set of thruster electrical operating conditions, the cathode flow rate could be increased by increasing the current through the magnetic baffle control coil. The values of magnetic baffle current chosen (up to 15 A) allowed stable thruster operation. For the entire series of tests the neutralizer was operated at a constant keeper current of 2 A with a flow rate of approximately 60 mA.

Three current transformer probes were used to sense the discharge current, beam current, and neutralizer keeper current fluctuations (time-varying component of the current). These probes were placed around the appropriate current-carrying conductors from the power supplies to the thruster. The discharge voltage fluctuations were measured by using a current probe to sense the current through a 1000-ohm noninductive resistance connected across the discharge supply leads. For further details on the probes and data systems and their calibration, refer to Fig. 1 and Ref. 6. Also given in Ref. 6 is a brief description on the method of analyzing the time-varying data which include the rms magnitudes, spectral data and correlation measurements.

Results and Discussion

This section will present the results of the rms magnitude, spectral data, and correlation measurements, in that order.

Received March 5, 1975; presented as Paper 75-345 at the AIAA 11th Electric Propulsion Conference, New Orleans, La., March 19-21, 1975; revision received June 7, 1976.

Index categories: Plasma Dynamics and MHD; Electric and Advanced Space Propulsion; Spacecraft Propulsion Systems Integration.

*Aerospace Engineer, Aerodynamics Analysis Section, Propulsion Aerodynamics Branch. Member AIAA.

†Aerospace Engineer, Large Thruster Section, Electric Propulsion Branch.

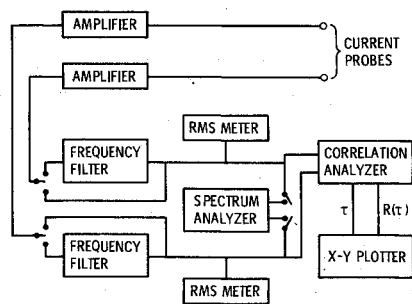


Fig. 1 - Schematic diagram of instrumentation used to obtain cross-correlations and spectra for plasma fluctuations.

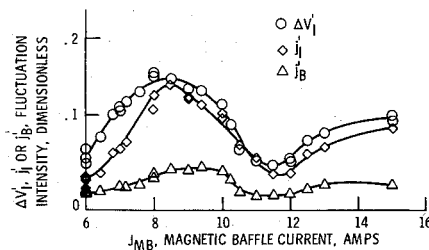


Fig. 2 - Effect of varying the magnetic baffle current on the fluctuation intensity of the discharge current and voltage and ion beam current, $J_B = 2.0$ A, $\Delta V_i = 37.0$ V, and $J_i = 12.0$ A.

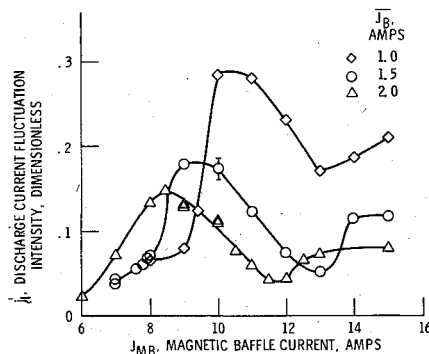


Fig. 3 - Effect of varying the magnetic baffle current on the fluctuation intensity of the discharge current for $J_B = 1.0, 1.5,$ and 2.0 A with $\Delta V_i = 37.0$ V.

RMS Magnitudes

Figure 2 shows the fluctuation intensity, the ratio of the rms magnitude to the time-average currents for the beam current and discharge voltage and current as a function of J_{MB} , the magnetic baffle current, for a J_B of 2.00 A, ΔV_i of 37.0 V, and a J_i of 12.0 A. The lowest value of J_{MB} in Fig. 1 (6.0 A) was the lowest value at which the thruster subsystem could be operated stably. In Fig. 2 the fluctuation intensity curves for the discharge current and voltage are nearly identical whereas the curve for the beam fluctuations has a magnitude considerably lower than the other two curves over the measured range of J_{MB} . The intensity of the discharge current and beam current fluctuations are lower than those given in Ref. 6.

The behavior of the fluctuation intensity as a function of J_{MB} suggests that several different plasma modes are experienced over this range of J_{MB} . Further information on this point will be discussed subsequently in the section on spectral data. Similar behavior of the fluctuation intensities as a function of J_{MB} were found in Ref. 6 which further emphasizes the possibility that, over this range of J_{MB} , there exist several plasma modes. The shapes of the curves presented here are similar to those of Ref. 6 but are not identical. The lack of identity possibly might be attributed to the differences in the interactions of the thruster plasmas with their power supplies

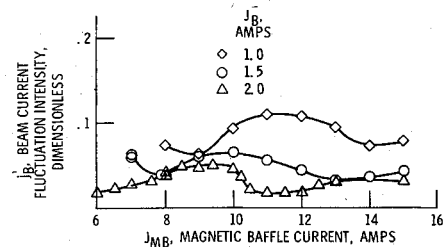


Fig. 4 - Effect of varying the magnetic baffle current on the fluctuation intensity of the beam current for $J_B = 1.0, 1.5,$ and 2.0 A with $\Delta V_i = 37.0$ V.

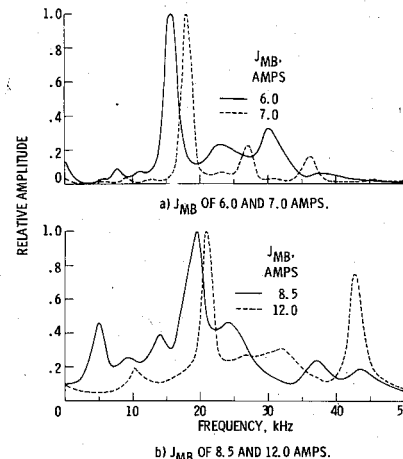


Fig. 5 - Effect of various magnetic baffle currents on the relative amplitude as a function of frequency for the discharge current fluctuations with $J_B = 1.0$ A, $J_i = 12.0$ A, and $\Delta V_i = 37.0$ V.

or the differences in discharge chamber geometry and magnetic field. For the work reported in Ref. 6, the thruster (a "400 series"), modified only by the addition of dished ion optics, was powered by a high-frequency transistor inverter-type console.

Figure 3 compares the fluctuation intensity for the discharge current as a function of J_{MB} for J_B values of $1.0, 1.5,$ and 2.0 A. The variation of the fluctuation intensity with magnetic baffle current for J_B values of 1.5 and 1.0 A is similar to that for a beam current of 2.0 A. The values of J_{MB} at which the maxima occur increases as J_B is increased. Near the maxima of the curves there was a low-frequency amplitude modulation of the fluctuation intensity. It was most severe for a J_B value of 1.5 A. The range of values of the fluctuation intensity existing under these conditions is shown in Fig. 3 by an error bar (± 0.015) at J_{MB} of 10 A (J_B of 1.5 -A curve).

Figure 4 compares the fluctuation intensity of the beam current, as a function of J_{MB} for a J_B of $1.0, 1.5,$ and 2.0 A. The effect of varying J_B is generally similar to that observed in Fig. 3. As J_{MB} is decreased to the minimum value, however, the beam current fluctuation intensity does not continue to decrease for J_B of 1.5 and 1.0 A as in the case of J_B of 2.0 A. In fact, for a J_B of 1.5 A, the average value of the beam current fluctuation intensity at minimum J_{MB} is 0.060 , which is nearly as great as the maximum of the curve (0.064) occurring at a higher J_{MB} .

The effect on the fluctuations of varying the discharge current as beam currents were held constant can be found in Ref. 13 (an expanded version of this paper). Also given there is the effect of varying the discharge voltage with all other thruster parameters maintained at their nominal operating values.

The neutralizer keeper current and flow rate were not varied throughout the entire series of tests. With J_{NK} , the

time-average neutralizer keeper current, of 2.0 A, the fluctuation intensity, j'_{NK} , was 0.068 ± 0.001 .

Spectral Data

Two types of spectral data will be presented in this section. First, in Fig. 5 the amplitude spectra of the discharge current fluctuations are presented for a J_B of 2.0 A for a range of values of J_{MB} . For these spectral data, the fundamental frequency F_0 and the harmonic set of frequencies (F_1, F_2, F_3, \dots), along with their corresponding relative amplitudes ($A_0, A_1, A_2, A_3, \dots$) are summarized in Table 1 (which also presents these data for J_B of 1.5 and 1.0 A). The second type of spectral data is given in Fig. 6 which gives the relative log amplitude of the fluctuations of beam current, neutralizer keeper current, and discharge current and voltage as a function of frequency for a given thruster operating condition.

Figures 5a and 5b show the relative amplitude of the discharge current fluctuations as a function of frequency up to 50 kHz at a J_B of 2.0 A for several values of J_{MB} . Looking at the spectrum for any given value of J_{MB} reveals that the spectrum up to 50 kHz has a number of peaks including a major one (always having a relative amplitude value of 1.0 by definition). Inspection of the spectrum for J_{MB} of 6.0 in Fig. 5a shows that the major peak does not occur at the lowest or fundamental frequency. It occurs at 15.6 kHz. There is a smaller peak at a frequency of 7.7 kHz. The oscillation is occurring at the first harmonic frequency, not the fundamental, and there also are smaller peaks at 23.0, 30.0, and 37.6 kHz which could be those occurring at the second, third, and fourth harmonic frequencies (Table 1a). For a J_{MB} of 7.0 A in Fig. 5a there is a similar behavior. For both curves of Fig. 5a there are also other smaller peaks which are not included in this harmonic set.

The data for a J_{MB} value of 8.5 A in Fig. 5b reveal that the major peak occurs at a frequency of 19.3 kHz, and a harmonic set now has only frequencies of 9.8 and 19.3 kHz, corresponding to the zeroth and first harmonic frequencies, respectively. Peaks occurring at frequencies other than this harmonic set plainly are evident for this value of J_{MB} and they occur at 5.0, 13.7, and 23.9 kHz. The curve for a J_{MB} value of 12.0 A reveals that the major peak occurs at a frequency of 20.8 kHz and the harmonic set (as shown in Table 1a) now has frequencies of 10.2, 20.8, 32.0, and 43.0 kHz. Two points to note about the data for a J_{MB} value of 12.0 A are 1) the lack of smaller peaks other than the harmonic set and 2) the fact that the third harmonic peak at 43.0 kHz has a large relative amplitude of 0.75. Consideration of the frequencies of the major peaks in both Figs. 5a and 5b shows that this frequency increases nonlinearly with the J_{MB} .

Spectral data for the fluctuations resulting from varying the discharge current and voltage were taken but will not be presented here (nor in Ref. 13). However, the behavior of the main peak of the spectra is considered. The frequency of the major peak was found to vary nonlinearly with J_I and linearly with ΔV_I .

Considerable analysis will be required to develop models adequately explaining both the details of these spectra and the fluctuation intensity results such as given in Table 1 and Fig. 5 as well as in Refs. 6 and 13. Even before that can be done, however, additional information on the dynamics of the plasma in the ionization chamber will have to be obtained. It also will be necessary to analyze the dynamic characteristics of the power supplies for the thruster and to consider possible interactions of thruster and power supply.

Despite the complexity of the spectra, some possibilities as to their physical origin should be considered as was done in Ref. 14 for the fluctuations observed with an 8-cm ion engine. Simple physical consideration reveal that, of the resonances or oscillations observed in similar plasmas, three possibilities that can be considered here are ion-acoustic resonances, resonances due to $\mathbf{E} \times \mathbf{B}$ particle drifts, and resonances due to effects of anomalous diffusion. Without a more complete knowledge of the plasma properties of 30-cm discharge chamber plasmas, it will not be possible to compare quantitatively the frequencies of observed peaks with the calculated values. However, by making some appropriate assumptions and estimates for the plasma parameters, at least a qualitative comparison can be presented herein for the ion-acoustic resonance (see Refs. 13 and 14 for a more complete discussion of these resonances).

The ion-acoustic resonance can be calculated by using $v_{th} = (kT_e/M_i)^{1/2}$ for the characteristic velocity; where T_e is the electron temperature and M_i is the mass of the mercury ion. A characteristic frequency is determined from v_{th}/ℓ ; where ℓ is a characteristic length in the discharge. If a T_e of 5 eV and a ℓ of 15 cm (half-diameter of the 30 cm thruster) are assumed, then the characteristic frequency obtained is 10.3 kHz. How T_e varies with the operating conditions is not known. Also, the validity of the characteristic length assumption may be questioned. However, these estimates of the ion-acoustic resonant frequencies appear to be in reasonable agreement with the results presented in Fig. 5 and Table 1.

Figure 6 compares the spectra of the fluctuations of the discharge current and voltage, the neutralizer keeper current and beam current. Figure 6 gives the spectra with the relative amplitude in decibels as a function of frequency in hertz (plotted on a log scale) for a range of frequencies to 450 kHz. The thruster operating conditions for the data of Fig. 6 are J_B equal to 2.0 A, J_I equal to 12.0 A, ΔV_I equal to 37.0 V, and

Table 1 Amplitudes and frequencies of spectral peaks for discharge current fluctuations

J_{MB}	F_0 , kHz/ A_0	F_1 , kHz/ A_1	F_2 , kHz/ A_2	F_3 , kHz/ A_3	F_4 , kHz/ A_4	F_5 , kHz/ A_5
a) $J_B = 2.0$ A						
6.0	7.7/0.09	15.6/1.00	23.0/0.23	30.0/0.33	37.6/0.06	
7.0	8.9/0.04	18.0/1.00	27.1/0.22	36.5/0.16		
8.5	9.8/0.26	19.3/1.00		37.3/0.22		
12.0	10.2/0.20	20.8/1.00	32.0/0.31	43.0/0.75		
b) $J_B = 1.5$ A						
7.0	10.3/1.0	20.4/0.70	30.3/0.25	41.2/0.13		
9.0	8.0/0.15	15.7/1.0	23.5/0.24	39.5/0.07		
11.0	8.6/0.69	17.0/0.95	25.5/1.00	33.8/0.98	42.3/0.67	
15.0	20.9/1.0	41.7/0.47				
c) $J_B = 1.0$ A						
8.0	9.8/1.0	19.4/0.47	29.2/0.25	38.8/0.25		
9.0	4.7/0.12	9.1/1.0	13.5/0.27	17.8/0.57	22.3/0.55	
10.0	6.3/0.45	12.3/1.0	18.7/0.49	30.0/0.16		
12.0	4.7/0.41	8.0/1.0	14.5/0.71	20.5/0.57	28.5/0.39	
15.0	6.7/0.57		18.5/1.0			36.3/0.395

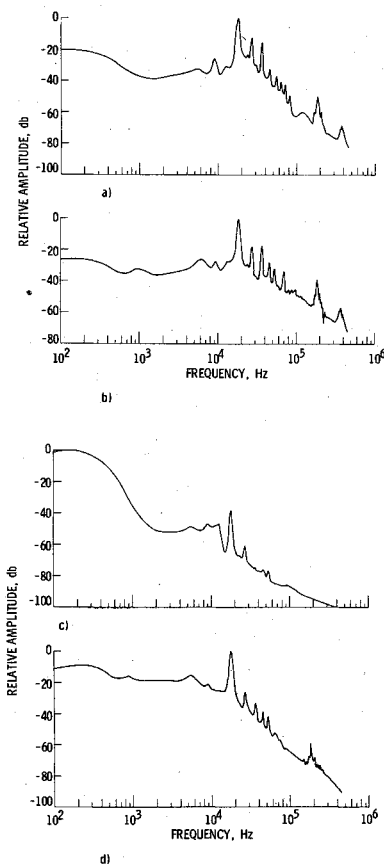


Fig. 6 Relative amplitude in decibels as a function of frequency for $J_B = 2.0$ A, $J_I = 12.0$ A, and $\Delta V_I = 37.0$ V. a) For the discharge current fluctuations. b) For the discharge voltage fluctuations. c) For the neutralizer keeper current fluctuations. d) For the beam current fluctuations.

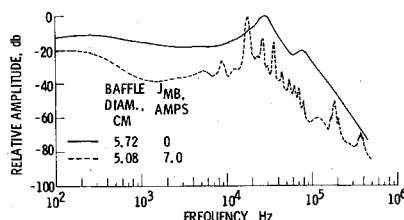


Fig. 7 Comparison of the relative amplitude in decibels as a function of frequency for the discharge current fluctuations for two different baffle diameters, $J_B = 2.0$ A, and $\Delta V_I = 37.0$ V.

J_{MB} equal to 7.0 A. This value of J_{MB} at a J_B of 2.0 A represents a stable mode of the thruster at a minimum cathode flow rate. Figure 6a gives the spectrum for the discharge current fluctuations. As previously noted, the main peak is at a first harmonic frequency of 18 kHz and there are other harmonic frequencies in evidence in consecutive order up to 81 kHz.

The relative amplitude at frequencies from 100 to 200 Hz is about -20 dB and may be indicative of the effect of the power supply low-frequency ripple on the fluctuations of the discharge chamber plasma. No such indication was found in Ref. 6, which presents a spectrum of the discharge current fluctuations, taken with J_B at 1.0 A and J_{MB} at 13.0 A. The power conditioning console used contained 10- and 5-kHz inverters rather than 60-Hz laboratory supplies. In Ref. 6, for frequencies greater than the main-peak frequency, the falloff in amplitude with increasing frequency was found to be 45 dB per decade. Because of the multiplicity of peaks in Fig. 6a the falloff in amplitude with increasing frequency is determined by a locus of the minima between the peaks. This gives a slope

of about -48 dB per decade. This reasonable agreement with Ref. 6 suggests that the power supply differences may not be important at the higher frequencies for the fluctuations in discharge current.

Figure 6b presents the spectrum of the fluctuations of the discharge voltage. Its shape is generally similar to that for the discharge current fluctuations. The spectrum in Fig. 6b has, as expected, a similar set of peaks at the same frequencies as Fig. 6a. For frequencies greater than the main-peak frequency, the falloff in amplitude with increasing frequency is about 32 dB per decade, which is considerably less than that for the discharge current fluctuations.

The spectrum of the neutralizer keeper current fluctuations is given in Fig. 6c. The main peak of this spectrum is in the 100–200 Hz frequency range. The next highest peak has a relative amplitude of -38 dB and is at 17.5 kHz. In Ref. 6, the spectrum of the neutralizer keeper current fluctuations consisted entirely of discrete peaks of a harmonic set with the fundamental frequency being 5.4 kHz, the inverter frequency. Thus, these two spectra are quite dissimilar.

Figure 6d presents the spectrum of the beam current fluctuations. The main peak is at a frequency of 18 kHz and, as was found for the discharge chamber fluctuations in Figs. 6a and 6b, can be considered as the first harmonic of a harmonic set. In evidence in Fig. 6d is the peak at 180 kHz with a relative amplitude of -59 dB. Similar peaks were observed in the spectra of the discharge voltage and current fluctuations. At frequencies greater than the main-peak frequency the falloff in relative amplitude with increasing frequency is -48 dB per decade. Thus, the spectrum of the beam fluctuations appears to depend on the spectrum of the discharge chamber fluctuations. In addition the spectrum of the beam fluctuations appears to depend on the neutralizer fluctuations in the lower frequency range. Looking at the low-frequency part of Fig. 6d, it is seen that the relative amplitude is as high as -9 dB and this appears to be related to the main peak of the spectrum of the neutralizer keeper current fluctuations. The apparent dependence of the beam fluctuation spectra on the discharge fluctuations is a result also found in Ref. 6. Although the spectra of the neutralizer keeper current fluctuations are dissimilar in Fig. 6c and Ref. 6, in both cases there is an effect on the beam fluctuation spectra.

Because the size of the baffle used has a strong effect on the J_{MB} cathode flow rate relation, it should be expected to alter not only the time-average discharge characteristic but also the time-varying properties of the discharge. Figure 7 compares the spectra of discharge current fluctuations for baffle diameters of 5.08 and 5.72 cm. Results for the 5.08-cm-diam baffle, taken from Fig. 6a, are presented in Fig. 7 as a dashed curve. The solid curve presents data for the 5.72-cm-diam baffle at J_{MB} of 2.0 A (both curves represent a stable, low cathode flow rate). This comparison in Fig. 7 illustrates clearly the significant change in the spectrum of the discharge fluctuations that can result from the slight change in baffle size. In the case of the spectrum for the 5.72-cm baffle diameter, there are only two peaks with frequencies at 29 and 78 kHz. The lower peak may be a second harmonic of the higher one. However, the frequency ratio is 2.7. Because the error in determining the frequency is hardly sufficient to say 2.7 is equivalent to 3.0, these two peaks are probably the result of two different physical resonance phenomena. Both peaks are broader than those for the smaller size baffle. The falloff in amplitude at the higher frequencies is about 65 dB per decade for the larger baffle diameter. This is a significantly greater falloff than was obtained for the smaller baffle size as in Ref. 6.

Correlations of the Fluctuations

A limited set of cross-correlations of the thruster fluctuations was obtained (see Ref. 13 for discussion of cross-correlations). Correlation curves were obtained in terms of R , the correlation coefficient, as a function of τ , the time delay

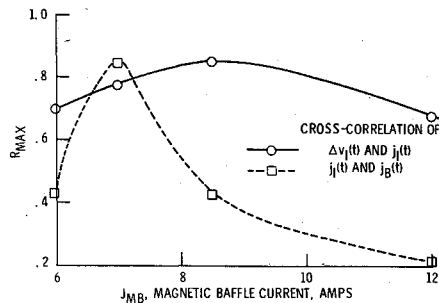


Fig. 8 Variation of R_{\max} , maximum cross-correlation coefficient, as a function of magnetic baffle current, J_{MB} , for $J_B = 2.0$ A, $\Delta V_I = 37$ V, and $J_I = 12.0$ A.

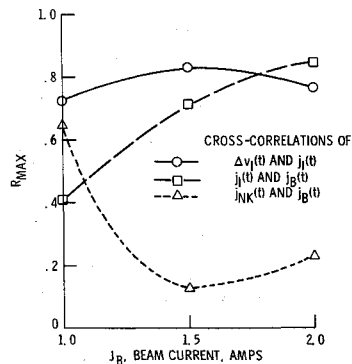


Fig. 9 Variation of R_{\max} , maximum cross-correlation coefficient, as a function of the beam current, J_B , for $\Delta V_I = 37.0$ V and minimum cathode flow rates.

between the fluctuations. Figure 8 presents R_{\max} , the maximum correlation coefficient, as a function of J_{MB} , the magnetic baffle current, for a J_B equal to 2.0 A. The solid curve in Fig. 8 is for the cross-correlation of the fluctuations of discharge voltage and current. As the magnetic baffle current is varied from 6.0 to 12.0 A, there is a rather slight variation in R_{\max} over a significant range of J_{MB} . Also, the values of R_{\max} are rather high (R_{\max} equal to 1.0 is the greatest possible value). This simply indicates that the fluctuations in discharge voltage and current are a consequence of the same physical phenomena.

The dashed curve in Fig. 8 is for the cross-correlation of the fluctuations of the discharge and beam currents. As the magnetic baffle current was varied from 6.0 to 12.0 A, the value of R_{\max} increased from 0.43 to 0.85 and then decreased to 0.21. This rather wide variation in the values of R_{\max} suggests that the dependence of the beam fluctuations on the discharge current fluctuations is strongest at the lower J_{MB} values and is less elsewhere.

Figure 9 presents R_{\max} , the maximum correlation coefficient, as a function of J_B , the beam current. The solid curve in Fig. 9 is for the cross-correlations of the fluctuations of discharge voltage and current. As J_B varies from 1.0 to 2.0 A, there is a slight variation in R_{\max} . The high values of R_{\max} simply indicate, as previously noted, that the fluctuations in discharge voltage and current are a consequence of the same physical phenomena.

The dashed curve with square data symbols in Fig. 9 is for the cross-correlations of the fluctuations of the discharge and beam currents. As the beam current increases from 1.0 to 2.0 A, the R_{\max} increases from 0.42 to 0.89. Because all of these data are taken at the lowest cathode flow rate consistent with the stable operation of thruster subsystem, the increase in R_{\max} as J_B increases is dependent on the J_{MB} values. In Ref. 6 the opposite trend of R_{\max} with increasing J_B was obtained. This difference in the behavior of R_{\max} with J_B has to be attributed to the differences in thruster geometry and power

conditioning console in the two situations. It would be of interest to perform these experiments using a given thruster powered by several different power conditioning consoles.

The small-dashed curve with triangular data symbols in Fig. 9 is for the cross-correlations of the fluctuations of the neutralizer keeper and beam currents. For beam currents of 1.5 and 2.0 A, the R_{\max} values are small and agree with those obtained in Ref. 6. This lack of high correlation is in agreement with the fact that the two spectra are dissimilar in shape (i.e., for J_B of 2.0 refer to Fig. 6). The rather high value, 0.69 for R_{\max} at J_B of 1.0 is probably indicative of the low-frequency fluctuations of the neutralizer keeper supply having a significant effect on the spectrum of the beam fluctuations. Thus, the cross-correlation of these two fluctuations would have a high value of R_{\max} . This increase in R_{\max} at J_B of 1.0 is contrary to the results of Ref. 6 wherein the R_{\max} values ranged from 0.12 to 0.14 for J_B from 1.0 to 2.0 A.

Concluding Remarks

An experimental investigation of the fluctuations of the discharge and beam plasmas of a 30-cm ion thruster has been performed. The power supplies were of the 60-Hz laboratory-type. Studied were a range of beam currents, J_B , from 1.00 to 1.00 A and a range of magnetic baffle currents, J_{MB} , from 6.0 to 15.0 A. Also studied were a small range of discharge currents and voltages about the optimum values for thruster operation at an energy expenditure of 185 eV per ion and a discharge voltage of 37.0 V. The results include the following:

- 1) The intensity of the fluctuations was found to depend significantly on the beam and magnetic baffle currents and the dependence on the latter current indicated that there were several plasma modes in evidence across the range of magnetic baffle current.
- 2) The shape of the spectra of the discharge plasma fluctuations was found to depend on both the beam and the magnetic baffle currents, but primarily on the latter and the dependence on the magnetic baffle current and beam current was found to be complex.
- 3) The predominant amplitudes of the spectra of the beam and discharge currents occurred at frequencies less than 30 kHz and the discharge chamber resonance possibly could be attributed to an ion-acoustic wave phenomenon.
- 4) The cross-correlations of the discharge and beam currents indicated that the dependence on the magnetic baffle current was strong and highest at a magnetic baffle current about 1 A above that required for minimum cathode flow rate and stable thruster operation.
- 5) The cross-correlations of the fluctuations of the discharge and beam currents and the neutralizer keeper and beam currents were found to depend on the time-average beam current.
- 6) The results of the spectral and cross correlation measurements indicate a) that the discharge current fluctuations directly contribute to the beam current fluctuations and b) that there is some evidence that the power supply characteristics affect the fluctuations.

References

- 1 Duxbury, J. H., "An Integrated Solar Electric Spacecraft for the Encke Slow Flyby Mission," AIAA Paper 73-1126, Lake Tahoe, Nev., 1973.
- 2 Gilbert, J. and Guttman, C. H., "The Evolution of the SEP Stage/SEPS/Concept," AIAA Paper 73-1122, Lake Tahoe, Nev., 1973.
- 3 Masek, T. D., Richardson, E. H., and Watkins, C. L., "Solar Electric Propulsion Stage Design," AIAA Paper 73-1124, Lake Tahoe, Nev., 1973.
- 4 "Thermoelectric Outer Planets Spacecraft (TOPS)," Jet Propulsion Laboratory, Pasadena, Calif., JPL-TM-33-589, April 1973; also NASA CR-131451, 1973.
- 5 Gardner, J. A., "Solar Electric Propulsion System Integration Technology (SEPSIT). Volume 1: Technical Summary," Jet

Propulsion Laboratory, Pasadena, Calif., JPL-TM-33-583-Vol. 1, Nov. 1972; also NASA CR-130701, 1972.

⁶ Serafini, J. S. and Terdan, F. F., "Plasma Fluctuations in a Kaufman Thruster," *Journal of Spacecraft and Rockets*, Vol. 11, Nov. 1974, pp. 752-758; also AIAA paper 73-1056, 1973.

⁷ Serafini, J. S., "Correlation Measurements of Plasma Fluctuations in a Hall-Current Accelerator," *Bulletin of the American Physical Society*, Vol. 13, Feb. 1968, p. 278.

⁸ Serafini, J. S., "Utility of Conventional Turbulence Experimental Methods in the Study of Plasma Fluctuations," *Bulletin of the American Physical Society*, Vol. 13, May 1968, p. 824; also NASA TMX-52371, 1967.

⁹ Serafini, J. S., "Measurement of the Coherent Oscillations and Turbulence in Plasma Using Resistively and Capacitively Coupled Probes," NASA TMX-1975, 1970.

¹⁰ Sovey, J. S. and King, H. J., "Status of 30-cm Mercury Ion Thruster Development," AIAA Paper 74-1117, San Diego, Calif., 1974.

¹¹ Mantenieks, M. and Rawlin, V. K., "Studies of Internal Sputtering on a 30-cm Thruster," AIAA Paper 75-400, New Orleans, La., 1975.

¹² Finke, R. C., Holmes, A. D., and Keller, T. R., "Space Environment Facility for Electric Propulsion Systems Research," NASA TN D-2774, 1965.

¹³ Serafini, J. S., Mantenieks, M. A., and Rawlin, V. K., "Dynamic Characteristics of a 30-cm Mercury Ion Thruster," AIAA Paper 75-345, New Orleans, La., 1975.

¹⁴ Serafini, J. S. and Nakanishi, S., "Measurements of Plasma Fluctuations in a 8-cm Mercury Ion Thruster," AIAA Paper 75-396, 1975, New Orleans, La.

¹⁵ Wilbur, P. J., "Hollow Cathode Restartable 15 cm Diameter Ion Thruster," Dec. 1973, Colorado State Univ., Fort Collins, Colo.; also NASA CR-134532, 1973.

From the AIAA Progress in Astronautics and Aeronautics Series . . .

IONIZATION IN HIGH-TEMPERATURE GASES—v. 12

Edited by Kurt E. Shuler, National Bureau of Standards, and John B. Fenn, Princeton University

The thirteen papers in this volume summarize present knowledge in ionization in high temperature gaseous systems, covering elementary processes, ionization in flames, in shock and detonation waves, in rocket exhausts, and electron generation by seeding.

Thermodynamics studies examine the state-of-the-art, with still-remaining problems, covering ion-molecule reactions, chemi-ionization in rare gases, flame ionization, proposing a mechanism for ion formation, charge transfer, recombination, and ambipolar diffusion.

Ionization behind strong shock waves, in detonation waves, and in exothermal and endothermal waves, is also studied, together with investigations of rocket exhaust ionization, both primary and secondary, with directions for future research.

Seeding studies concern use of alkali salts in combustion gases, with mechanisms for prediction and measurement of effects. Experimental studies of seeded gases cover the use of many elements in seeding for magnetohydrodynamic power generation, and the use of metal powders detonated in the upper atmosphere to enhance electron density for over-the-horizon radio transmission.

409 pp., 6 x 9, illus. \$10.00 Mem. & List

TO ORDER WRITE: Publications Dept., AIAA, 1290 Avenue of the Americas, New York, N. Y. 10019